

AD-A071 527

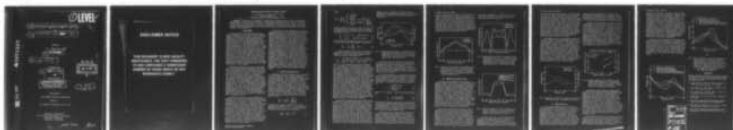
STANFORD UNIV CALIF MICROWAVE LAB
TRANSDUCER ARRAYS SUITABLE FOR ACOUSTIC IMAGING, (U)
SEP 75 C S DE SILETS, J FRASER, G S KINO
ML-2482

F/G 17/1

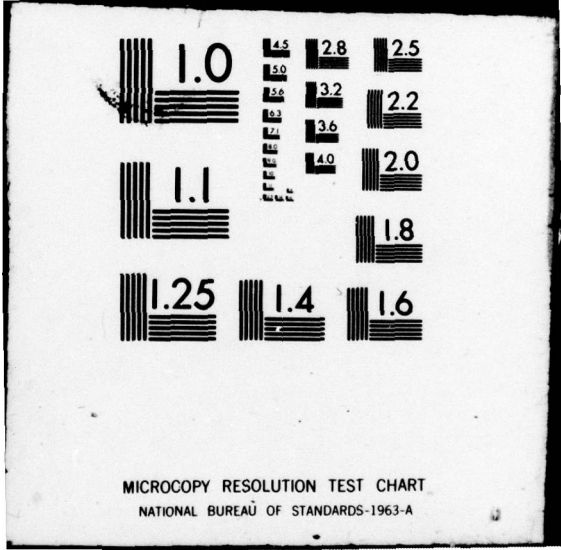
UNCLASSIFIED

N00014-75-C-0632
NL

| OF |
AD
A071527



END
DATE
FILMED
8 -79
DDC



① LEVEL II

⑥ TRANSDUCER ARRAYS SUITABLE FOR ACOUSTIC IMAGING

by

⑩ C. S. De Silets, J. Fraser ~~██████████~~ G. S. Kino

SC

ADA 071527

Preprint

M. L. Report No. 2482

⑪ Sep. ~~██████████~~ 1975

⑭ ML-2482

Contract No.

⑮ ~~NSF-14-75-C-0632~~
✓ NSF-GK-24635

DDC
RECEIVED
JUL 24 1979
B

DISTRIBUTION STATEMENT A
Approved for public release;
Distribution Unlimited

⑫ 17p.

DDC FILE COPY

Presented at

1975 IEEE Ultrasonics Symposium

held at

Los Angeles, September 22-24, 1975

Microwave Laboratory
W. W. Hansen Laboratories of Physics
Stanford University
Stanford, California

229 750

Jim

79 06 20 154

DISCLAIMER NOTICE

THIS DOCUMENT IS BEST QUALITY PRACTICABLE. THE COPY FURNISHED TO DDC CONTAINED A SIGNIFICANT NUMBER OF PAGES WHICH DO NOT REPRODUCE LEGIBLY.

C. S. De Silets, J. Fraser, and G. S. Kino
 Microwave Laboratory
 Stanford University, Stanford, California 94305

ABSTRACT. Progress on the development of piezoelectric transducer arrays for use in electronically focused acoustic imaging systems is reported. Design techniques and experimental results are described for two types of transducer arrays, one utilizing individual slotted array elements, and the other, array elements constructed by depositing electrodes on a monolithic slab of piezoelectric ceramic. Development of lossy, high impedance tungsten-epoxy matched backing material, necessary for broad bandwidth transducer arrays, is also described.

I. Introduction

A progress report on our development of piezoelectric transducer arrays for use in acoustic imaging systems is presented in this paper. These arrays are formed of a large number of small piezoelectric elements bonded to a lossy, matched impedance backing. Several severe requirements have been imposed on these arrays, which are: (1) high electromechanical conversion efficiency, (2) broad bandwidth operation of at least 50% bandwidth, so they can be excited over a wide range of frequencies or with short pulses, (3) an acceptance angle of $\pm 15^\circ$ in some cases and as much as $\pm 30^\circ$ in others for large aperture electronic focusing systems, (4) small cross-coupling between the array elements in order that transducer elements can be excited separately or to insure large angle of acceptance in a phased array, and (5) short signal decay times in the array elements and backing so that the same array can be used for both transmission and reception. In addition, ease and cost of fabrication of the arrays is an important consideration since ultimately two dimensional electronically focused imaging systems might use arrays with as many as 10,000 elements.

The design techniques for two types of 60 element linear arrays which have been tested in an electronically focused imaging system are described here. These arrays are designed to have 1.27 cm long elements with a 1.27 mm center-to-center spacing. They are soldered down to a lead backing, which has an impedance of 22×10^5 cgs Rayls where PZT-5A has an impedance of 34. Individual elements of rectangular cross-section, constructed by diamond sawing through a slab of PZT-5A already bonded to the lead backing, is utilized in one type of array. The cross-coupling between the elements is minimized by the physical separation of the elements. A high effective $k_t^2 = 0.477$ has been obtained in these structures. The center frequency and the 70% bandwidth obtained in short test arrays are determined by choosing the elements to have a suitable cross-sectional configuration and by the use of a matched backing.¹ A broad angle of acceptance of $\pm 32^\circ$ has been obtained in short test arrays by keeping the width of element less than a wavelength in water.

A second kind of array has been constructed by depositing metal electrodes by standard photolithography techniques onto a slab of piezoelectric material mounted on a matched, lossy backing.^{2,3} Electrical cross-coupling between the elements is minimized by depositing ground electrodes in between the elements of the array. A $\pm 16^\circ$ acceptance angle limited by the longitudinal wave critical angle between water and PZT-5A ceramic is obtained by acoustic impedance matching with a thick lead backing. An acceptance angle of $\pm 25^\circ$ for this type of array has been obtained by using a lower velocity piezoelectric ceramic, lead metaniobate. The PZT-5A array on a lead backing has given a 50% bandwidth. The k_t^2 of this type of array is about one-half that of the slotted array. However, this array is potentially most useful in high frequency applications or for large two-dimensional arrays with very many elements where fabrication problems are most severe.

In both kinds of arrays described, the transducer characteristics are largely determined by the acoustic impedance matching of the piezoelectric material to a high loss, high impedance backing material. An adequate backing for both kinds of arrays has been provided by soldering PZT-5A or lead metaniobate ceramic with Ni - Cr electrodes to lead, which has an acoustic impedance of 22 and a plane wave loss of 3.2 dB/cm at 2 MHz. However, since the loss mechanism in lead appears to be caused by scattering into incoherent sound waves which themselves have very slow decay rates, the dynamic range of an array with elements serving as both receiving and transmitting transducers or with interlaced receiving and transmitting transducers is severely limited. Tungsten-loaded epoxy backings have higher loss and much faster multimode decay rates. Consequently, these backings allow greater receiver sensitivity and dynamic range than lead backings. Results of experiments with tungsten-loaded epoxy backings are reported in which high acoustic impedance material up to $Z_B = 10$ with plane wave loss of at least 10 dB/cm in $Z_B = 24$ material have been fabricated. Techniques to minimize the effect of the bond thickness between the ceramic and the backing are reported as well as results with a simple large area transducer to test the bonding procedures and basic theory.

II. Slotted Transducer Arrays

Experiments have been carried out with lead-backed PZT-5A transducers in which the poling direction (z-axis) corresponds to the thickness dilatational mode of large area plates. These transducers have been slotted so that the width (W) of the element (x-axis) is comparable to the height (H) of the element (z-axis). The length (L) of the element (y-axis) is large compared to the width and the height. In the case where $W \leq 0.6H$, a theory has been carried out from which the electrical impedance of the transducer elements has been predicted. As long as the width of the element is fairly small compared to the height, it is assumed that there is no longitudinal stress in the x direction, or $T_1(x,z) = 0$. In the nonpiezoelectric case, the effective stiffness constant is calculated, assuming $T_1 = 0$, to be

$$c_{33}^E = c_{33}^E \left(1 - \frac{c_{13}^E c_{13}^E}{c_{11}^E c_{33}^E} \right) \quad (1)$$

By applying this boundary condition to the piezoelectric case, assuming $D_z(x,z) = 0$ and open circuit conditions so that $D_z(x,z) = 0$, a piezoelectrically stiffened elastic constant can be obtained

$$c_{33}^D = c_{33}^E (1 + k^2) \quad (2)$$

where

$$(k')^2 = \frac{e_{33}^2}{C_{33}^E c_{33}^S} \frac{\left(1 - \frac{e_{13}^2 C_{11}^E}{C_{11}^E c_{33}^S}\right)^2}{\left(1 + \frac{e_{13}^2}{C_{11}^E c_{33}^S}\right)} + \frac{e_{13}^2}{C_{11}^E c_{33}^S} \left(1 - \frac{C_{13}^E}{C_{11}^E c_{33}^S}\right)^2 \quad (3)$$

Using the modified relations for C_{33}^E , C_{33}^D , and k'^2 , and substituting in the physical constants of PZT-5A,¹ the lowered effective stiffened velocity and impedance are calculated to be

$$\bar{v}'_a = \bar{v}_a (1 + k'^2) = 3.78(10)^5 \text{ cm/sec} \quad (4)$$

$$\bar{Z}'_a = \rho_{mo} \bar{v}'_a = 29.3(10)^5 \text{ cgs Rayls} \quad (5)$$

The electromagnetic coupling constant k_T^2 is found to be 0.477 and the zero strain dielectric constant is

$$\epsilon_{33}^S = \epsilon_{33}^S + \frac{e_{13}^2}{C_{11}^E} = 857 \epsilon_0 \quad (6)$$

Using the effective values of the transducer constants in the standard three-port model of a backed transducer,⁵ the electrical input impedance of the transducer element is determined to be

$$Z = \frac{1}{j\omega C'_0} + \frac{k_T'^2}{\omega C'_0 \bar{\beta}'_a H} \left[\frac{(Z_B / \bar{Z}'_a) \sin \bar{\beta}'_a H + 2j(1 - \cos \bar{\beta}'_a H)}{\sin \bar{\beta}'_a H - j(Z_B / \bar{Z}'_a) \cos \bar{\beta}'_a H} \right] \quad (7)$$

where C'_0 is the effective zero strain capacitance, $\bar{\beta}'_a$ is the effective stiffened propagation constant, H is the height of the element, and Z_B is the backing material impedance. The calculated electrical impedance of a lead-backed PZT-5A transducer element 0.635 mm high, 0.381 mm wide, and 12.73 mm long is compared to the magnitude and phase of the electrical impedance of the transducer in Fig. 1. It is assumed that the effective impedance of the lead is 22 as in the infinite case, although variational analysis theories lead us to believe that the effective impedance seen by a finite element should be higher than this value. With this assumption, excellent agreement between the experimental and theoretical impedance phase angle as a function of frequency is observed. The shape of the impedance magnitude as a function of frequency also shows excellent agreement, but there is a 30% level shift in magnitude. This level shift is felt to be attributable to an overall scale factor which appears to be due to a lower value of the zero-strain capacitance than would be predicted from the manufacturer's values for c_{33}^S or the measured values of ϵ_{33}^S in larger samples of the same material. As will be seen from the figures, broad bandwidth response of the transducer is obtained.

For transducer element widths nearly equal to element heights, the simplifying assumption of zero stress in the x direction is no longer valid and a sharp transverse resonance peak with relatively small damping appears; this gives a double-peaked electrical impedance response and consequently narrow bandwidth. Thus, square cross-section transducers should be avoided if broadband operation is desired. Transducer elements of this type, where the width is much greater than the height, will also give broadband operation in the thickness dilatational mode since the transverse mode resonance will be much lower in frequency than the thickness dilatational mode. However, care must be exercised in the use of such elements if a wide acceptance angle is desired since the acceptance angle will be small if the width of element is several times the acoustic wave-

length in water. Furthermore, the stress fields in this mode are nonuniform and the coupling to them tends to be weak if the elements are only one or two wavelengths wide.

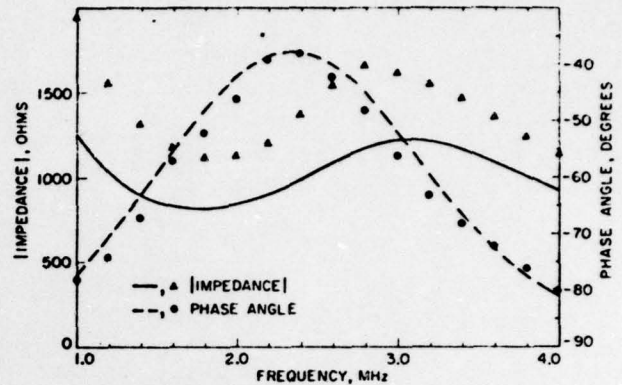


FIG. 1--Comparison of theoretical vs experimental electrical impedance of slotted test array element. Element size is 0.381 mm wide, 0.635 mm high, 1.27 cm long. Test array is built of variable element width lead-backed PZT-5A.

For these reasons, the element cross-section for the final 60-element array used in the electronically focused system of elements was designed to be 0.635 mm high and 0.381 mm wide. Two elements on 0.635 mm center-to-center spacing were connected in parallel to form one receiving or transmitting element. This design has the advantages of redundancy and high coupling obtained with tall elements.

The angular acceptance of a slotted transducer element is easily obtained from integration over the width of the transducer of the phase variation of a constant amplitude plane wave incident at an angle θ to the surface normal. The output voltage for a plane wave of unit amplitude incident on the transducer is found to be

$$V = k \frac{\sin\left(\frac{\pi W}{\lambda} \sin \theta\right)}{\frac{\pi W}{\lambda} \sin \theta} \quad (8)$$

where k is a constant. So the 3 dB acceptance angle is

$$\theta_a = \sin^{-1} \left[\frac{1.39 \lambda}{\pi W} \right] \quad (9)$$

The theoretical angular acceptance of a single backed 0.635 mm wide transducer 1.092 mm high in an array with a period spacing of 1.191 mm is compared in Fig. 2 with the measured angular acceptance at 2 MHz. The agreement is fairly good, and the acceptance angle continues to be wide over a broad frequency range.

The deviation from the theoretical prediction for angle of acceptance appears to be caused by cross-coupling to adjacent array elements. If the coupling is very strong, the transducer array appears to be a simple wide transducer with a concomitant narrow angle of acceptance for each element. Thus, acceptance angle measurements yield a good, if indirect, measure of the amount of cross-coupling between narrow array elements.

In Fig. 2, the size of the peaks at 0° , and $\pm 23^\circ$ can be reduced simply by short-circuiting the adjacent elements. The origins of the cross-coupling seen in these arrays are not completely understood, but at present, it is certain that the interstices between array elements should be free of high dielectric constant material like water. There is also evidence that waves can propagate along a thick continuous surface layer which is bonded to the face of the array and so strongly couple the elements together. Further work is necessary in this area, and it is clear that cross-coupling can be a severe problem in these transducer arrays.

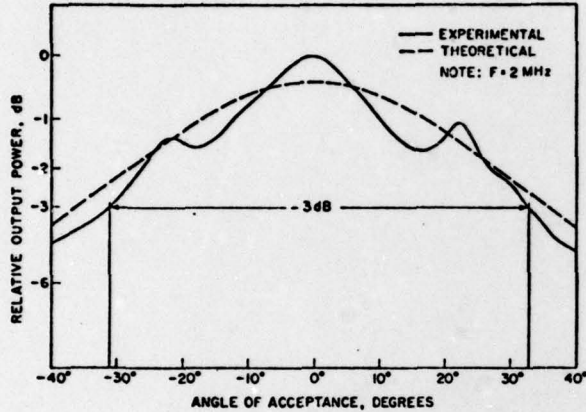


FIG. 2--Comparison of theoretical vs experimental relative output power $P(\theta)$ as function of angle of acceptance of slotted test array element. Element size is 0.635 mm wide, 1.092 mm high. Test array is built of lead-backed PZT-5A with 1.194 mm element spacing.

III. Monolithic Transducer Arrays

A second type of transducer array suitable for acoustic imaging, which utilizes an acoustically matched monolithic slab of piezoelectric ceramic onto which individual electrodes have been deposited to form individual array elements, has been previously described.^{2,3} The results of experiments with a five-element array constructed by soldering 1.092 mm thick PZT-5A onto a thick lead backing have verified the basic theory of the device. In this case, the array elements were constructed by depositing 38 mm long, 0.279 mm wide Cr-Au electrodes on 1.524 mm centers onto the face of the ceramic slab. In addition, a 60-element device has been constructed using 0.635 mm PZT-5A soldered onto a thick lead backing. This array, like the slotted array, has been successfully used as an interlaced 30-element focused transmitter and 30-element focused receiver in a B-scan imaging system and as a 30-element focused transmitter in a C-scan transmission imaging system.⁶

This array is operated on the principle, that by impedance matching the piezoelectric ceramic slab to lower the Q of the resonator and to prevent plane wave reflection at the matched face of the resonator, the angle of acceptance will approach the longitudinal critical angle of the ceramic. The theory of the point response of the resonator as a function of angle and frequency has been previously described. A comparison of theoretical output power $P(\theta)$ of the five-element test array to the measured output power with adjacent electrodes shorted is shown in Fig. 3. Note that the width of the element electrode is chosen to be small

compared to a wavelength at 2.7 MHz so that the angular response is unaffected by the phase variation across the width of the electrode.

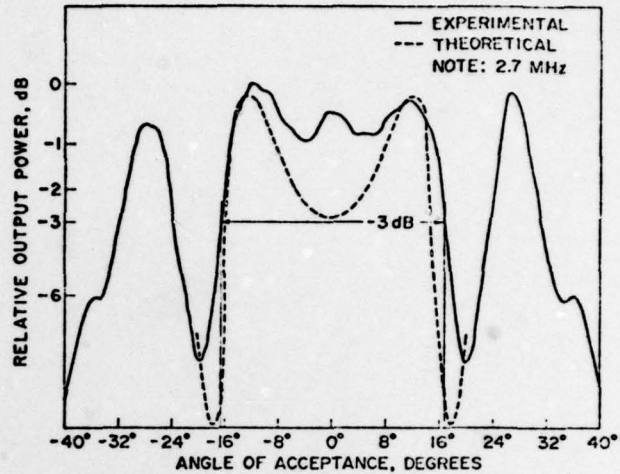


FIG. 3--Comparison of theoretical vs experimental relative output power $P(\theta)$ as function of angle of acceptance of monolithic test array element. Element size is 0.279 mm wide, 3.81 cm long. Test array is built of 1.092 mm thick lead-backed PZT-5A with 1.524 mm element spacing.

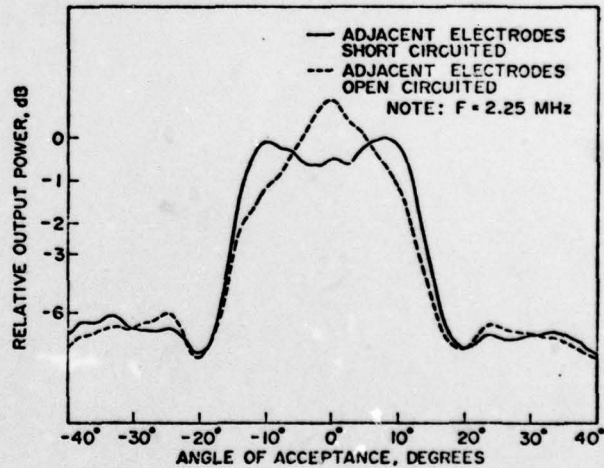


FIG. 4--Effect of grounding adjacent elements on the relative output power $P(\theta)$ as function of angle of acceptance of monolithic test array element. Same dimensions as in Fig. 3.

As can be seen in Fig. 3, the agreement between the theoretical and measured angular responses is quite good. The measured response, however, has a pronounced peak at 0° incidence which appears to be caused by capacitive coupling to the ceramic material surrounding the element electrode which is not predicted

by the present point response theory. As can be seen in Fig. 4, the effect of shorting out some ceramic material near the element under test, achieved by short-circuiting the adjacent electrodes, reduces this capacitive pick-up considerably. Shorting of all the material around the electrode further reduces this pick-up, and the measured response compares more closely to the predicted point response. The sixty element B-scan array utilizes thin ground electrodes between the array elements to reduce this pick-up. Further work has indicated that large ground electrodes between the array elements will be necessary in order that this measured angular response will compare closely to the predicted point response. However, a more uniform response as a function of angle can in fact be obtained with the grounded electrodes between the elements.

The bandwidths of the array elements reported here are 50% as expected by the simple impedance matched transducer theory. The electrical impedance of a test array element is shown in Fig. 5. The flatness of the impedance characteristics is excellent and is much flatter than predicted by a simple matched transducer theory in which the only coupling term is assumed to be ϵ_{33}^S . The measured impedance is almost unaffected by shorting out the adjacent electrodes. Further work is necessary to predict the electrical impedance of the array element correctly taking into account the ϵ_{31}^S coupling terms on the nonuniform fields in the transducer as well as to correctly predict the cross coupling effects. However, broadband, high acceptance angle monolithic transducer arrays can be constructed which perform adequately in acoustic imaging systems.

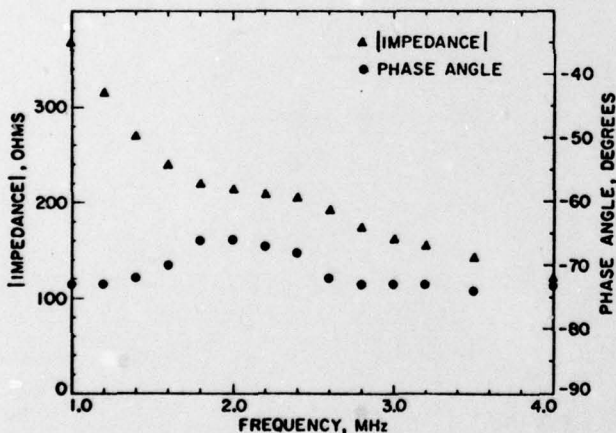


FIG. 5--Experimental electrical impedance of monolithic test array element. Same dimensions as Fig. 3.

IV. Backing Materials

A lossy, high impedance backing material and a suitable technique for attaching it to a transducer are of prime importance in the construction of broadband transducer arrays. Lead has an acoustic impedance of 22, and has been used as a backing, with the bond achieved by soldering. Good acoustic contact was achieved, and it was thought that the attenuation in lead would be sufficient. The plane wave attenuation in lead at 2 MHz was measured as 3.0 dB/cm, but it was found that this attenuation is principally due to scattering rather than absorption, and that the slowly decaying scattered sound in the backing of a transducer array severely limits the receiver sensitivity and

dynamic range when operating in a reflection mode. This is because transmitted pulses propagate into the backing and are scattered into strong incoherent signals which appear as excess noise on the array's electrical outputs during reception of the desired signal.

In order to obtain a backing material of similarly high impedance, but far greater loss, tungsten-epoxy composites have been fabricated. An aggregate of tungsten particles of average size 50 microns is pressed to the desired density, and the interstices are filled by vacuum impregnation with a low viscosity casting epoxy, Dow Epoxy Resin #332. Impedances in the range of 8.5 to 40 have been produced, and impedances in the range of 20 to 30 have been reproducibly achieved. Samples of impedance 24 have been found to have loss greater than 10 dB/cm at 2.7 MHz. Figure 6 shows the velocities and impedances obtained by pressing the powder before epoxy impregnation to obtain various final densities. Tungsten-epoxy backings may be glued to transducers with the same thin epoxy used to fabricate them, or may be cast in place.

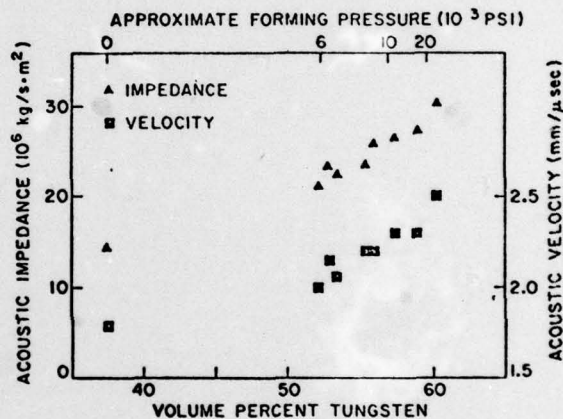


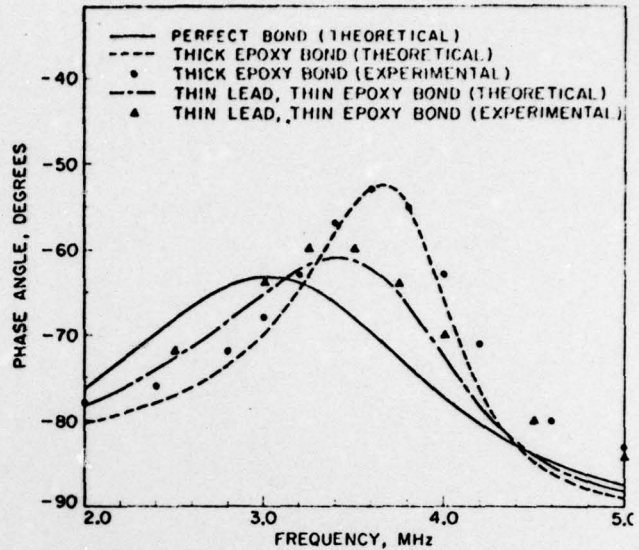
FIG. 6--Acoustic impedances and velocities of some tungsten-epoxy composites. The approximate pressure required to achieve the given volume fractions of tungsten is also given. Tungsten particles of average size 50 microns.

To demonstrate the advantage of tungsten-epoxy over lead, nearly identical transducer assemblies were fabricated; one on lead, one on tungsten-epoxy of impedance 23. The transducers were PZT-5A plates, 0.635 mm thick and 7.5 mm by 10 mm laterally. The backings were cylindrical, 12.5 mm in diameter and 20 mm long. One transducer was soldered to the lead backing, and the other was cast in place on the tungsten-epoxy backing. The transducers were shock excited, and the decay rate of the output noise of the transducers was measured. The noise signal of the lead-backed transducer decayed at 0.5 dB/μsec, while that of the tungsten-epoxy backed transducer decayed at 3.8 dB/μsec, some 70 times faster. It is expected that tungsten-epoxy backings will eliminate the problem of backing noise in reflection mode operation of acoustic transducer arrays.

Good acoustic contact between a transducer and its backing is essential, and is not trivial to obtain with tungsten-epoxy. Two bonding methods have been used: gluing and casting in place. The quality of these methods has been evaluated by fabricating simple backed disc transducers and measuring their electrical

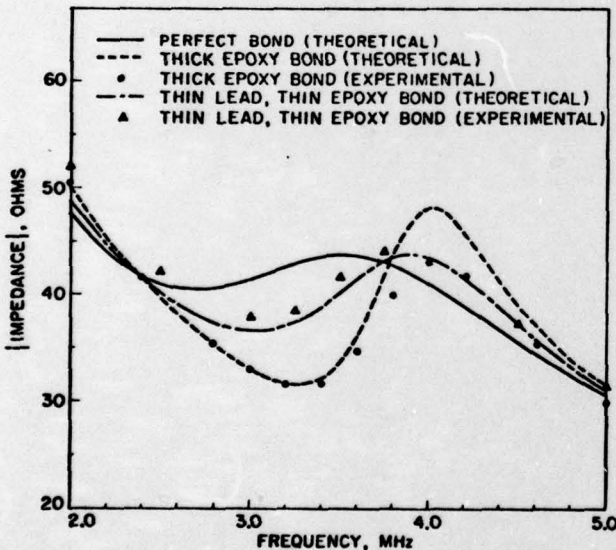
Impedances as functions of frequency. These measurements are compared with a theory which models the bonding layers as short transmission line sections. The effective thicknesses of the bonding layers are thus estimated. Figure 7(a) shows experimental data for the magnitudes of electrical impedance of two 0.635 mm thick PZT-5A transducers, normalized to one square centimeter area. Both are on tungsten-epoxy backings of impedance 23. One was epoxied on, the other tinned and cast in place. The purpose of the tinning was to provide a soft layer into which the tungsten particles could embed, improving the acoustic contact. For comparison, theoretical plots corresponding to a perfect, zero thickness bond; a 12.5 micron epoxy bond; and a two-layer, 15 micron lead - 5 micron epoxy bond are shown. Figure 7(b) gives the corresponding phase variations of the electrical impedances.

The cast in place transducer is sufficiently well bonded to possess 50% bandwidth, the value predicted by the Mason model⁷ for a perfectly bonded PZT-5A transducer on a backing of impedance 23. The phase of the acoustic output relative to the electrical input of one such transducer was measured at various frequencies by J. Souquet and was found to agree extremely well with that predicted by the same model. Cast in place tungsten-epoxy on a tinned transducer achieves adequate acoustic contact for acoustic transducer array applications.



(b)

FIG. 7--Effect of bonding on electrical impedance of a disc transducer. PZT-5A disc, 1 cm² area, 0.635 mm thickness, backing impedance 23. Theoretical plots for perfect, zero thickness bond; 12.5 μ epoxy bond; and 15 μ lead + 5 μ epoxy bond. Experimental points for epoxy glued bond and tinned and cast in place bond. (a) Magnitude of impedance; (b) Phase of impedance.



(a)

References

* The work reported in this paper was supported in part by the Office of Naval Research under Contract N00014-75-C-0632 and in part by the National Science Foundation under Grant 24635.

1. M. Onoe and M. F. Tiersten, IEEE Transactions on Ultrasonics Engineering, 10, 1, 32 (1963).
2. B. A. Auld, M. E. Drake, and C. G. Roberts, Appl. Phys. Letters 25, 479 (1974).
3. B. A. Auld, C. S. De Silets, and G. S. Kino, 1974 Ultrasonics Symposium Proceedings.
4. H. Jaffe and D. A. Berlincourt, Proc. IEEE 53, 10, 1372 (1965).
5. B. A. Auld, Acoustic Fields and Waves in Solids (Wiley, New York, 1973), Vol. I, Chapter 8.
6. G. S. Kino, C. De Silets, J. Fraser, and T. Waugh, 1975 Ultrasonics Symposium Proceedings.
7. W. P. Mason, Electromechanical Transducers and Wave Filters (Van Nostrand, Princeton, N.J., 1948).

ACCESSION for	
NTIS	White Section <input checked="" type="checkbox"/>
DDC	Buff Section <input type="checkbox"/>
UNANNOUNCED <input type="checkbox"/>	
JUSTIFICATION	
PER LETTER	
BY	
DISTRIBUTION/AVAILABILITY CODES	
Dist.	AVAIL. and/or SPECIAL
A	23